



Original scientific paper

Impact of manufactured sand and sintered fly ash aggregate on the mechanical and durability characteristics of normal-strength concrete

Ranjith Babu Baskaran^{*1)}, Nagarajan Divyah²⁾¹⁾ Department of Civil Engineering, PSNA College of Engineering and Technology, Dindigul. ORCID 0000-0002-4690-7834²⁾ Department of Civil Engineering, PSG Institute of Technology and Applied Research, Coimbatore. ORCID 0000-0001-5381-8226

Article history

Received: 26 April 2024

Received in revised form:

29 June 2024

Accepted: 03 July 2024

Available online: 30 August 2024

Keywords

sintered flyash aggregates,
mechanical properties,
impact strength,
M-sand,
durability studies

ABSTRACT

This study examined the impact of substituting Natural Coarse Aggregate (NCA) with varying quantities of sintered fly ash aggregate (SFA) in concrete. To ensure sustainability, manufactured sand (M-Sand) was consistently substituted for river sand in all mixtures. Slump values increased as the SFA content increased, which positively impacted workability. The results suggest that a complete replacement of the coarse aggregates can achieve substantial weight reduction potential. Even though compressive strength, split tensile strength, flexural strength, and Young's modulus decreased as the SFA content increased, all compositions (SFA0, SFA50, and SFA100) surpassed the minimum field requirement of 20 MPa compressive strength. Impact testing adversely affected the impact strength of the SFA50 mix, while SFA0 and SFA100 demonstrated comparable failure modes. It is important to note that replacing 50% NCA with SFA resulted in an increase in concrete durability, as demonstrated by a lower average sorptivity value. The results of this study indicate that SFA is a potential partial replacement for NCA. It provides advantages in terms of workability, weight reduction, and potential enhanced durability, while still maintaining adequate strength for field applications.

1 Introduction

Concrete construction has demonstrated the numerous advantages of using lightweight materials like sintered flyash aggregates, crushed clay bricks, and coconut shells. The advantages include possible cost savings, a decrease in autogenous shrinkage, and a reduction in concrete density when compared to ordinary concrete [1, 2 and 3]. Low bulk density, strong thermal insulation, and fire resistance are just a few of the benefits that make lightweight concrete a viable choice for both structural and non-structural building applications. The use of lightweight aggregates in concrete significantly reduces pouring costs.

The Sintered Flyash Aggregates (SFA) are produced with the help of flyash from thermal power plants mixed with 90 % water to convert in the form of pelletization and further, it is heated to produce lightweight aggregate. These sintered aggregates have an advantage in the construction industry in making structural lightweight concrete, arrestor beds, filter media, roof tiles, and land drainages [4]. Manufactured Sand (M-Sand) is made by crushing the hard granite stones into small, angular-shape particles that are washed and finely graded to be used as an alternative to river sand. The M-sand has almost an equal character as compared to river sand, which is less expensive and free from silt and clay particles [5].

The compressive strength of lightweight aggregates is never entirely dependent on porosity [6-7]. Several associated variables, such as changes in the mineralogical composition [8], the melting temperature of binders [9], the margin of densification during sintering [10], aggregate bloating [11], and internal flaws caused by thermal pressures [12], further influence the compressive strength. The recommended methods for designing concrete mixes for the development of Lightweight Aggregate Concrete (LWAC) differ greatly from standard approaches for designing aggregate concrete mixes [13]. The majority of mix design approaches, regardless of the aggregate properties and necessary strength, focus on fixing the paste volume of concrete or aggregate content [14]. This approach highlights the durability and strength of the material. Because lightweight aggregate is porous [15], it has a lower compressive strength capability and less free water in the paste matrix. Therefore, a substantial amount of cement paste is required to achieve optimal workability and strength. This might have an impact on the durability requirements of structural concrete.

The addition of sintered flyash aggregate strengthens the bond between the aggregate surfaces and cement paste [16, 17]. Extensive research is being carried out on the sustainable production of lightweight concrete using sintered flyash aggregates [18]. The researchers observed an

^{*} Corresponding author:E-mail address: ranjithbabucivil@psnacet.edu.in

increase in water absorption and voids as the proportion of sintered aggregates increased. Replacing 40% (by mass) of sintered flyash aggregate with 100% natural aggregates can increase the strength of the concrete [19]. Furthermore, reports indicate that using manufactured sand in ultra-high-strength concrete produces hydration products that are denser than those made with natural sand [20, 21].

The spherical shape of sintered flyash aggregate positively impacts the LWAC's workability. When comparing sintered flyash aggregates to regular angular aggregates, it is seen that a comparatively smaller amount of superplasticizer is needed to produce the required slump. Increased water-to-cement ratios or the use of plasticizer are suggested as ways to improve the workability of concrete made completely of manufactured sand [22]. Previous research revealed better compressive strength outcomes when compared to conventional aggregate concretes. It was also observed that the Interfacial Transition Zone (ITZ) has a major role in regulating the strength of the LWAC and that the strength of the aggregate alone does not influence the compressive strength of the concrete that is formed. When compared to regular concrete, variables such as test specimen size, loading rate, multi-axial stress, etc. have negligible effects in LWAC. Furthermore, it is noted that the correlations between cylinder and cube strength in standard concrete and LWAC differ.

Concrete's high permeability and capillary permeability primarily contribute to its durability. One such simple laboratory-based measurement, sorptivity, determines the durability index by measuring the amount of water that penetrates the concrete, and it holds practical significance. The lower the sorptivity value, the concrete will have a higher paste and a densified microstructure [16].

By analyzing the combined effects of Manufactured Sand (M-Sand) and Sintered Flyash Aggregate (SFA), this initiative pushes the limits of sustainable concrete production. The research successfully develops structurally lightweight concrete while simultaneously promoting resource conservation through the partial and complete replacement of natural river sand with SFA. This represents

a substantial contribution due to the potential cost savings and weight reduction benefits of lightweight concrete. The compressive strength, split tensile strength, flexural strength, Young's modulus, impact resistance against drop weight, and sorptivity of these samples are then experimentally examined. Overall, this study illuminates the potential of SFA and M-Sand as viable materials for sustainable construction applications, demonstrating encouraging outcomes in terms of strength, workability, and durability.

2 Experimental programme

2.1 Materials

The components utilized in creating the concrete mix were the following.

2.1.1 Cement

In this study, Ordinary Portland Cement (OPC) of 53 grade, produced by KPC Limited in India and meeting the IS:12269 standards [23], served as the binding agent. The laboratory assessed several properties of the cement, including specific gravity, fineness, setting time, and consistency, through various standard experiments as per the BIS code (IS 4031 Part 2, 4, 5, 11) [24-27]. Table 1 details the outcomes of these experiments.

2.1.2 Manufactured sand (M-sand)

The M-sand utilized in the concrete blend was procured from local suppliers in the vicinity. A grading analysis for the manufactured sand is in accordance with [28]. The sieve analysis graph in Figure 1 shows that the manufactured sand fits into Zone III of IS:383, and the particle size distribution is within the range of values given in IS:383. Additionally, the properties of manufactured sand are determined in accordance with BIS specifications [28, 29], which is enumerated in Table 2.

Table 1. Physical Properties of Cement Under Examination

Properties	Test results	Test method
Specific gravity	3.15	IS: 4031 (Part- 11) [27]
Fineness (m ² /kg)	320	IS: 4031 (Part- 2) [24]
Consistency (%)	33	IS: 4031 (Part- 4) [25]
Setting times (min)		IS: 4031 (Part- 5) [26]
(a) Initial setting time	52	
(b) Final setting time	300	

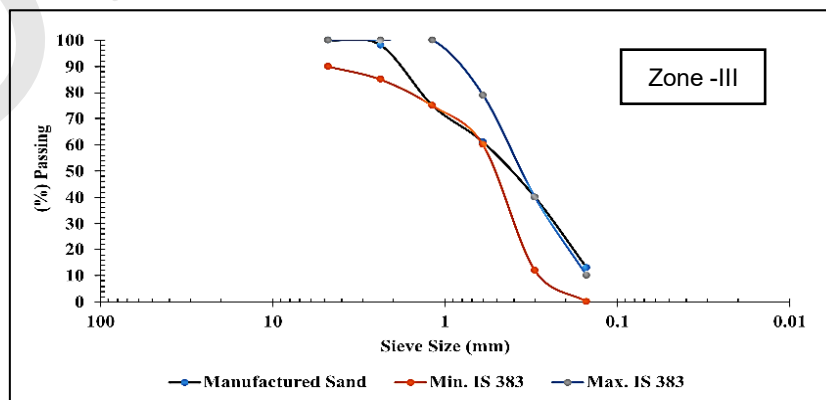


Figure 1. Gradation Curve for Manufactured Sand

Table 2. Physical Properties of Manufactured Sand

Properties	M-sand	Test method
Bulk density (Loose)	1632 kg/m ³	IS: 2386 (part -3) [29]
Bulk density (Compacted)	1797 kg/m ³	IS: 2386 (part -3) [29]
Specific gravity	2.5	IS: 2386 (part -3) [29]
Water absorption	0.4 %	IS: 2386 (part -3) [29]
Fineness modulus	2.14	IS: 2386 (part -1) [28]

2.1.3 Natural coarse aggregates (NCA)

The NCA used in the concrete mix was sourced from locally convenient suppliers. Grading analysis for coarse natural aggregates was carried out [28]. Figure 2 presents the sieve analysis graph. Table 3 also displays the properties of natural coarse aggregates determined according to BIS specifications [28, 29].

2.1.4 Sintered fly ash aggregates (SFA)

The SFA has been purchased from Ahmedabad, Gujarat, India, for use in the concrete mix. The SFA is spherical and brownish-grey, as seen in Figure 3. The various properties of SFA acquired in accordance with IS codal regulations are listed in Table 4. Table 4 shows that SFA was more capable of absorbing water than NCA. This increased water absorption influenced the porous nature of SFA. Figure 4 shows the sieve analysis graph and the grading analysis for sintered fly ash aggregate [28].

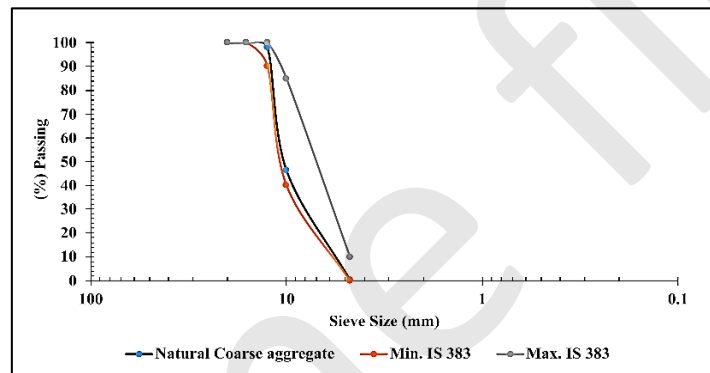


Figure 2. Gradation Curve for Natural Coarse Aggregates

Table 3. Tested Physical Properties of Natural Coarse Aggregates

Properties	NCA	Test method
Bulk density (Loose)	1467 kg/m ³	IS: 2386 (part -3) [29]
Bulk density (Compacted)	1640 kg/m ³	IS: 2386 (part -3) [29]
Specific gravity	2.4	IS: 2386 (part -3) [29]
Water absorption	1 %	IS: 2386 (part -3) [29]
Fineness modulus	2.6	IS: 2386 (part -1) [28]



Figure 3. Typical View of Sintered Fly ash Aggregates

Table 4. Physical Properties of Sintered Fly ash Aggregates

Properties	SFA	Test method
Bulk density - Loose	778 kg/m ³	IS: 2386 (part -3) [29]
Bulk density - Compacted	862 kg/m ³	IS: 2386 (part -3) [29]
Specific gravity	1.6	IS: 2386 (part -3) [29]
Water absorption	16.8 %	IS: 2386 (part -3) [29]
Fineness modulus	2.87	IS: 2386 (part -1) [28]
Impact value	27.78 %	IS: 2386 (part -4) [30]
Crushing value	15.63 %	IS: 2386 (part -4) [30]

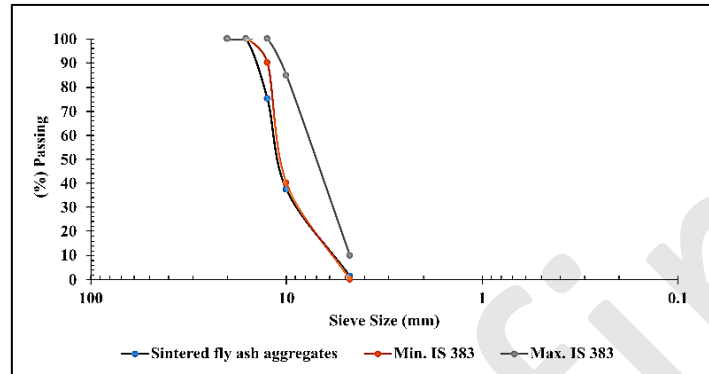


Figure 4. Gradation Curve for Sintered Fly ash Aggregates

2.1.5 Water

Portable water from the laboratory supply [31] was utilized in the production of this concrete mix.

2.1.6 Superplasticizer (SP)

Conplast SP430, a chloride-free additive based on sulfonated naphthalene polymers, was incorporated to enhance the workability of the concrete mix and serves as a water-reducing agent. All concrete mixes with a brown hue and a specific gravity of 1.22 received a dosage of 2% SP relative to the cement content.

2.2 Concrete Mix

The design of M30-grade concrete [32] used a control mix with a slump of 95 +/- 5 mm. Following the guidelines, coarse aggregates were utilized in Saturated Surface Dry (SSD) conditions for all mixes. Unlike SFA and NCA, where SFA exhibited a higher water absorption percentage, we maintained the water-to-cement ratio constant across all mixes. To achieve SSD conditions, additional water was introduced to the aggregate surfaces before mixing. SFA was substituted in the concrete mix by 50% and 100% of NCA, respectively, with the specific weight of the SFA serving as the primary parameter for coarse aggregate replacement. Table 5 provides detailed mix specifications.

Table 5. Mix details for concrete

Mix Designation	Replacement of NCA with SFA (%)	Cement (kg/m ³)	M - Sand (kg/m ³)	NCA (kg/m ³)	SFA (kg/m ³)	Water (kg/m ³)	SP(%)
SFA0	0	435	771	904	0	152.4	2
SFA50	50	435	771	301	301	152.4	2
SFA100	100	435	771	0	603	152.4	2

2.2.1 Casting and curing of specimens

The initial step in preparing the concrete mix involved dry-mixing the ingredients - cement, M-sand, NCA, and SFA - in the concrete mixer machine for three minutes. Subsequently, the dry mix was blended with water for five minutes to ensure uniformity in the concrete mixture. The concrete was poured into designated moulds, such as cubes, cylinders, prisms, and discs, after conducting a slump test to determine its consistency, and allowed it to set for 24 hours. Afterwards, the concrete samples were removed from the moulds and immersed in a concrete water curing tank until they reached the required curing age of 28 days. To facilitate various tests, specimens for each concrete mix were cast as follows.

- 3 nos. of 100 mm cubes both fresh and dry, were used to measure the compressive strength after 28 days.
- 3 nos. of 100 x 200 mm cylinders were tested for split tensile strength after 28 days.
- 3 nos. of 150 x 300 mm cylinders were used for Young's modulus test after 28 days;
- 3 nos. of 100 x 100 x 500 mm prisms were used for the determination of flexural strength after 28 days;
- 3 nos. of 150 x 64 mm discs were used for the determination of drop weight impact test after 28 days;
- 2 nos. of 100 x 50 mm discs were used for the determination of water sorptivity test after 28 days.

2.3 Testing Procedures

BIS and ASTM standards [33-37] were referenced to find various properties of the concrete specimens, including density (both fresh and dry), compressive strength, split tensile strength, flexural strength, Young's modulus, drop weight impact tests, and sorptivity tests.

3 Test results and discussion

3.1 Workability Measures

Figure 5 shows the change in slump values for different levels of SFA in concrete. Using M-sand in concrete instead of river sand reduces the slump value. The concrete mix without SFA has a lower slump value than the concrete mix containing 50% and 100% SFA. When SFA is replaced, the slump value increased by 55% and 73% compared to the concrete mix that does not contain SFA.

3.2 Wet and dry density

Figure 6 provides the change in the wet and dry density of the concrete mix. The concrete mix containing 0% SFA has a wet density of 2650 kg/m³. The addition of 50% and 100% SFA in the concrete mix reduced the wet density by 13% and 20%, respectively. A similar trend in the dry mix was

observed. The dry density of the concrete mix, which contains 0% SFA, is 2570 kg/m³. Further additions of 50% and 100% SFA in the concrete mix reduce the dry density to 14% and 19%, respectively. M-sand is used in all concrete mixes to increase wet and dry density. Concrete with a combination of light and normal weight aggregate [37] has a specific density greater than 2480 kg/m³ and can be defined as structural concrete.

3.3 Compressive Strength Test

Figure 7 displays the average test results of concrete cube samples after 28 days of normal water-curing. The 50% replacement of SFA in concrete reduces the compressive strength of the concrete by 17.14% and the 100% replacement of SFA reduces the compressive strength by 31.4%. The 100% SFA replacement signifies its structural lightweight nature, as its compressive strength is more than 21 MPa [37].

3.4 Split Tensile Strength

Figure 8 displays the 28-day split tensile strength values based on [34]. The increased SFA content in the concrete decreases the split tensile strength. 50% SFA in concrete decreases the split tensile strength by 27.2%, and 100% SFA in concrete decreases the split tensile strength by 20.3%.

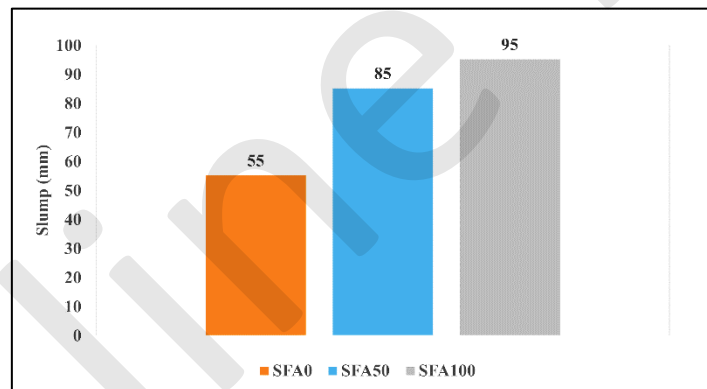


Figure 5. Variation of Slump Value for Different Levels of SFA In Concrete Mix

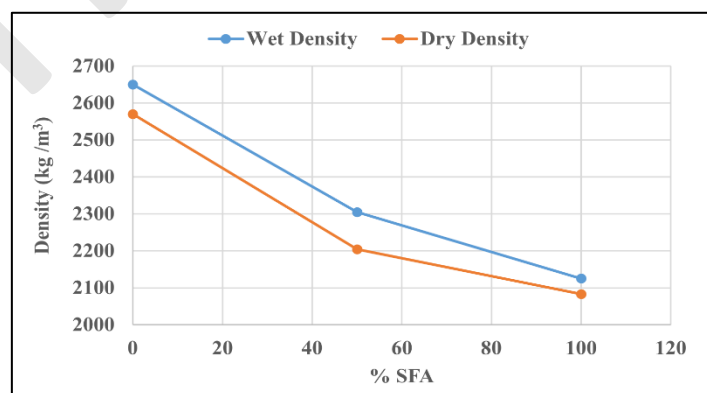


Figure 6. Wet And Dry Density of Concrete Mix Contains Varying SFA

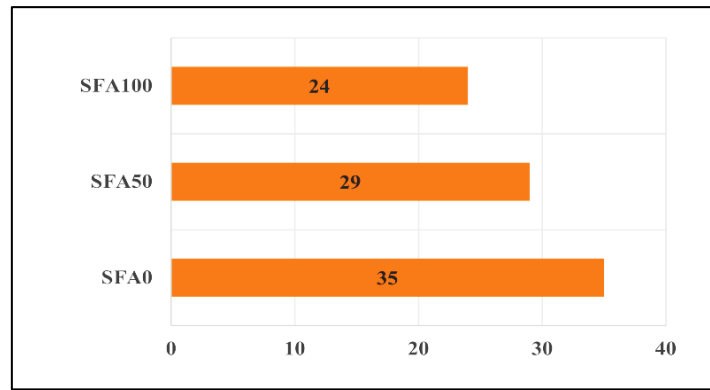


Figure 7. The Compressive Strength of Concrete Mix Contains Varying SFA

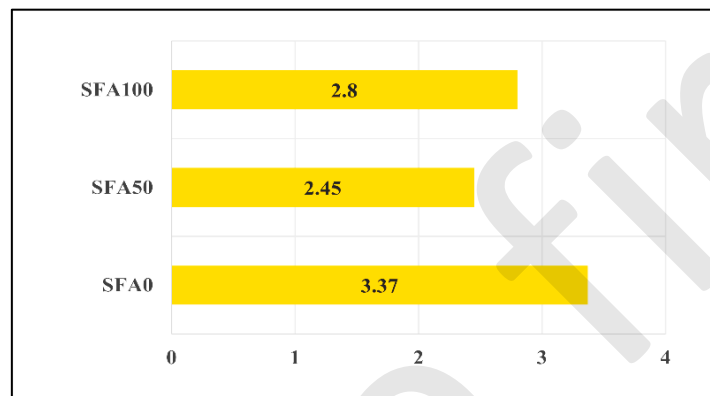


Figure 8. Split Tensile Strength of Concrete Mix Contains Varying SFA

Figure 9 illustrates the failure mode of tested split tensile cylindrical specimens. Various international codes were used [38–42] to compare the experimental values of split tensile strength. Table 5 provides the empirical formulas used for the prediction. The required cylinder compressive strength for the prediction of split tensile strength is calculated by multiplying 0.8 with cube compressive strength [43]. Figure 10 displays the predicted split tensile strength at 28 days using empirical formulas.

According to the ACI code regulation, replacing 50% of the coarse aggregate (SFA) in a concrete mix results in a split tensile strength that is higher than the strength of the tested samples. The observed values were greater than the projected values in the remaining codes. The drop in strength causes the SFA to rupture and pop out at 50% and 100% in the concrete mix [18]. The use of M-sand in concrete demonstrates its equivalence with river sand.

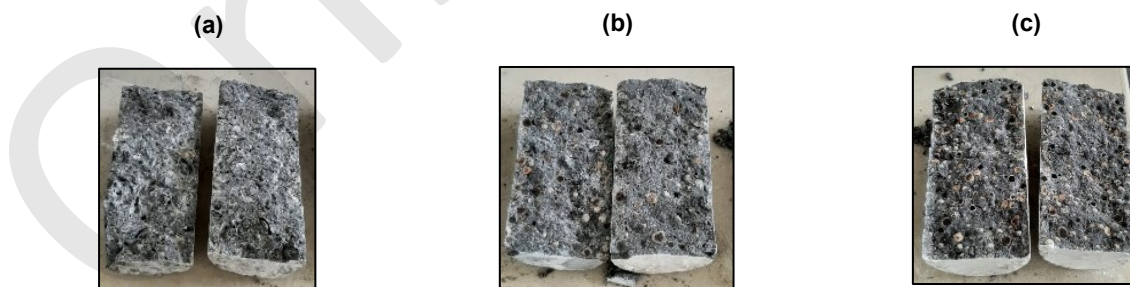


Figure 9. 28-Day Split Tensile Failure of Concrete Cylinders Contains SFA (a) 0% (b) 50% (c) 100%

Table 5. Formulas to Predict Split Tensile Strength (f_{sp}), Flexural Strength (f_{cr}), and Modulus of Elasticity (E) from Compressive Strength (f_c or f'_c)

Split tensile strength (f_{sp})	Flexural strength (f_{cr})	Modulus of elasticity (E)
$f_{sp} = 0.56\sqrt{f'_c}$ [38]	$f_{cr} = 0.62\sqrt{f'_c}$ [38]	$E = 4700\sqrt{(0.8f'_c)}$ [38]
$f_{sp} = 1.56\left[\frac{f'_c - 8}{10}\right]^{\frac{2}{3}}$ [39]	$f_{cr} = 0.70\sqrt{f'_c}$ [45]	$E = 5000\sqrt{f'_c}$ [45]
$f_{sp} = 0.21(f'_c)^{\frac{2}{3}}$ [40]	$f_{cr} = 0.81\sqrt{f'_c}$ [39]	$E = \left(\frac{100000}{2.8 + \frac{40.1}{f'_c}}\right)$ [44]
$f_{sp} = 0.19(f'_c)^{0.75}$ [41]	$f_{cr} = 0.75\sqrt{f'_c}$ [44]	
$f_{sp} = 0.19(f'_c)^{\frac{2}{3}}$ [42]		

Note: f_c and f'_c are 28-day cube and cylinder compressive strength, respectively.

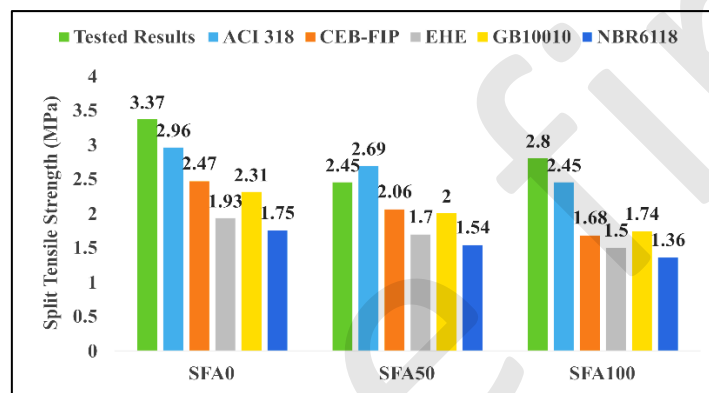


Figure 10. Comparison Between Predicted and Experimental Split Tensile Strength for The Concrete Mixture Containing Varying Percentages of SFA

3.5 Flexural Strength Test

The flexural strength was determined in the concrete cast [33]. Figure 11 depicts the variation in flexural strength at 28 days for concrete prisms made with an SFA-containing concrete mix. The flexural strength values exhibit a similar pattern to that observed in the split tensile and compressive strength data. For concrete mixes containing 50% and 100% SFA, respectively, the flexural strengths dropped by 25% and

14.8%. This decrease is caused by the addition of SFA to the concrete mix. The complete substitution results in a decrease in flexural strength of 14.8% when compared to a 50% SFA mixture. This suggests that a 100% SFA mixture exhibits the characteristics of lightweight concrete. Figure 12 depicts the failures of the evaluated flexural strength prism specimens.

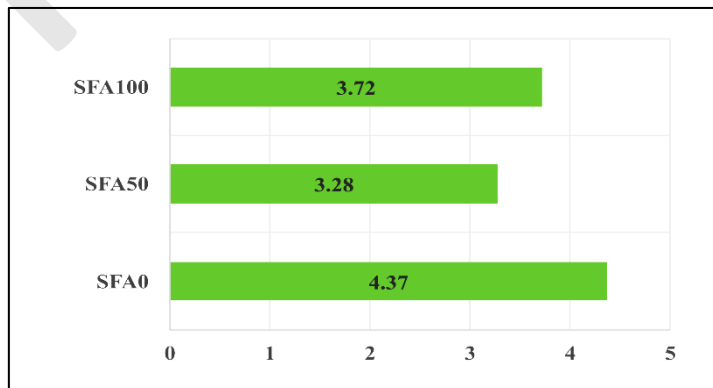


Figure 11. Flexural Strength of Concrete Mix Contains Varying SFA

The experimental flexural strength values were compared with various international codes available [38, 45, 39, 44]. Table 5 provides the empirical formulas used for predicting flexural strength. The formula suggests multiplying the cylinder's compressive strength by a factor of 0.8 by its corresponding cube compressive strength [43]. Figure 13 displays the predicted flexural strength results for the mix after 28 days. In comparison to the other codes, CEB-FIP predicts flexural strength with the highest accuracy. The flexural strength values for the concrete mix with 0% and 100% SFA predicted by the code DG/TJ demonstrate good agreement with experimental values. As the SFA content increased, the flexural strength values decreased. All concrete mixes contain M-sand, which had the similar properties as river sand.

3.6 Modulus of Elasticity

Figure 14 shows the variation of the 28-day tested secant modulus of elasticity (working stress) values, which are based on the cylindrical compressive stress-strain values. As the percentage replacement of SFA increased, the concrete mix's modulus of elasticity decreased. The split tensile and flexural strength values also follow the same trend.

The percentage decrease in secant modulus is 24.2% for SFA 50% and 46% for SFA 100. These reductions in elastic values are only due to the presence of SFA in the concrete mix. The modulus of elasticity determined experimentally is compared with various international codal provisions [38, 45, 44]. Table 5 lists the empirical values. Figure 15 displays the predicted values. The anticipated outcomes indicate that the

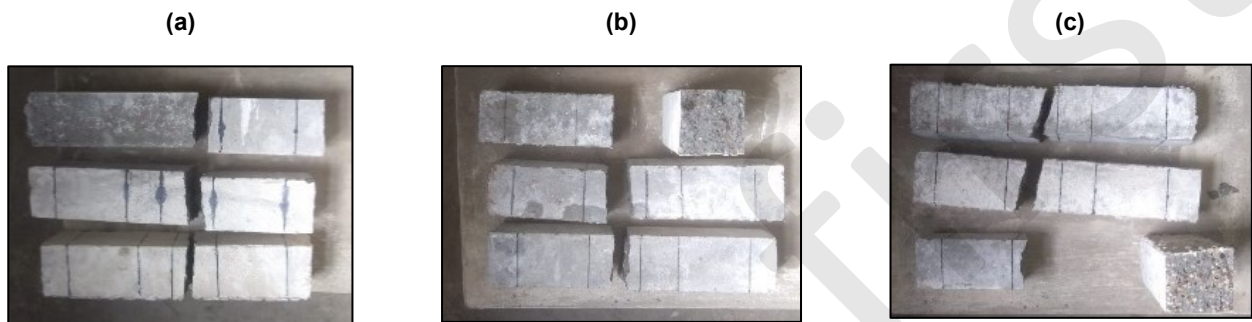


Figure 12. Flexural Failure of Concrete Prisms Contains. SFA (a) 0 % (b) 50 % (c) 100 %

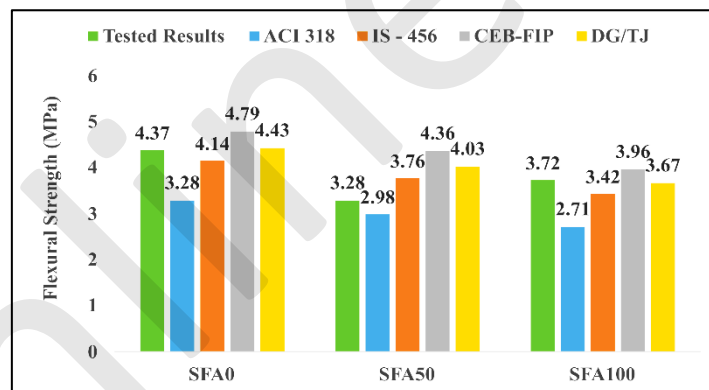


Figure 13. Comparison Between Predicted and Experimental Flexural Strength for The Concrete Mixture Containing Varying Percentages of SFA

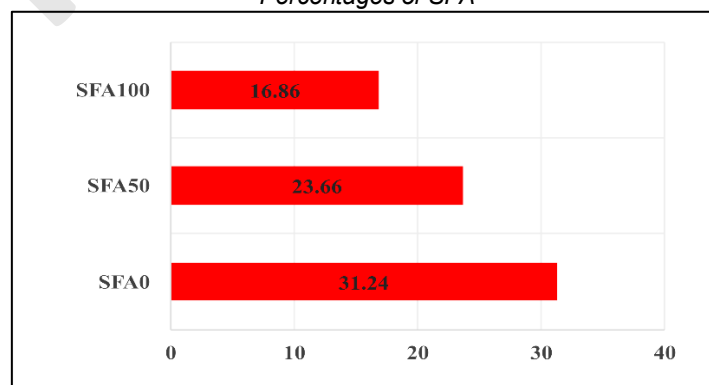


Figure 14. Modulus of elasticity of concrete mixture contains varying SFA

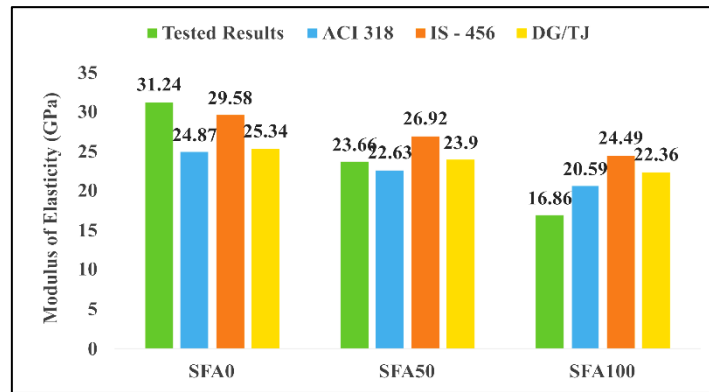


Figure 15. Comparison Between Predicted and Experimental Modulus of Elasticity for The Concrete Mixture Containing Varying Percentages of SFA

concrete mix comprising 50% and 100% SFA exhibits greater values compared to the experimental data. We observed that the IS 456:2000 code yields higher predictions than other codes. Unlike the SFA content, the use of M-sand in concrete shows no signs of degradation.

3.7 Drop Weight Impact Test

A simple drop weight test was used [46] to calculate the impact energy (J) of the concrete mix on nine 150-mm-diameter and 64-mm-high cylindrical specimens. Figure 16 displays the fabricated drop-weight impact tester. The test procedure follows: We released a 4.56 kg cylindrical mass, measuring 7 cm in diameter and 15 cm in height, from a height of 457 mm, and it collided with a 64 mm diameter steel ball that touched the top surface of the concrete specimens. The number of blows until the first crack appears (N1) is recorded. Then the test is continued until the cracks appear from bottom to top and the ultimate failure (N2) of the specimen is recorded.

The impact energy of each specimen was calculated using Equation [1]:

$$\text{Impact Energy (J)} = \left(\frac{mV^2}{2}\right) \cdot n = mgh \cdot n \quad [1]$$

The variables under consideration were V, m, g, n, and J. These variables represent the impact velocity, drop weight mass, acceleration due to gravity, number of blows to cause impact, and energy absorbed. Table 6 presents the findings of the 28-day impact energy test. The concrete mix using SFA50 has a comparable energy absorption capacity to that of the concrete mix without SFA (SFA0). The SFA100 mix had a 51.39% reduction in impact energy compared to the SFA0 concrete mix. A regression analysis was conducted on the concrete mix to examine the impact of adjusting the SFA content. The R-square values for the concrete mixes, including SFA0, SFA50, and SFA100, are 0.98, 0.99, and 0.99, respectively. Figure 17 depicts the regression chart for the concrete mix. Figure 18 depicts the failure mechanisms exhibited by the specimens under testing. The SFA50 concrete mix's failure mechanism aligns with the experimental study's observed failure mode [48].



Figure 16. Test Setup for Drop Weight Impact Tester

Table 6. Impact Resistance Results for the Concrete Mix Containing Varying Percentages of SFA

Mix Designation	N1 (mean)	N2 (mean)	N2-N1	N2/N1	J (Nm)	
					First crack	Final crack
SFA0	131	146	15	1.11	2678	2985
SFA50	142	148	6	1.01	2903	3026
SFA100	66	71	5	1.07	1349	1451

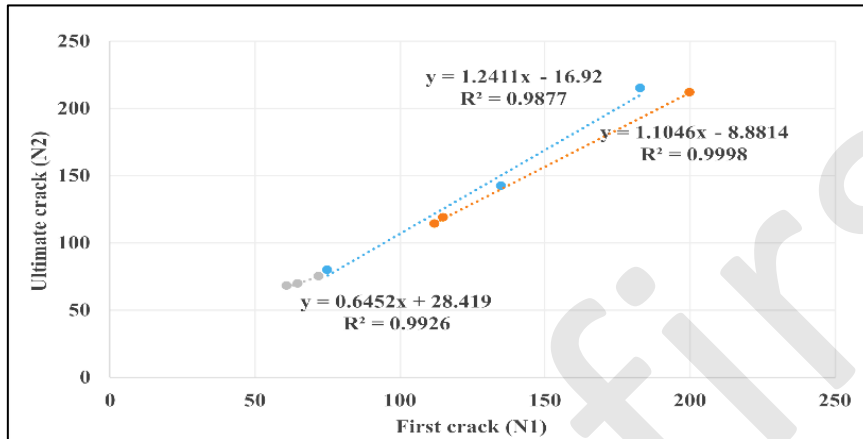


Figure 17. Regression analysis for the concrete mix for varying SFA

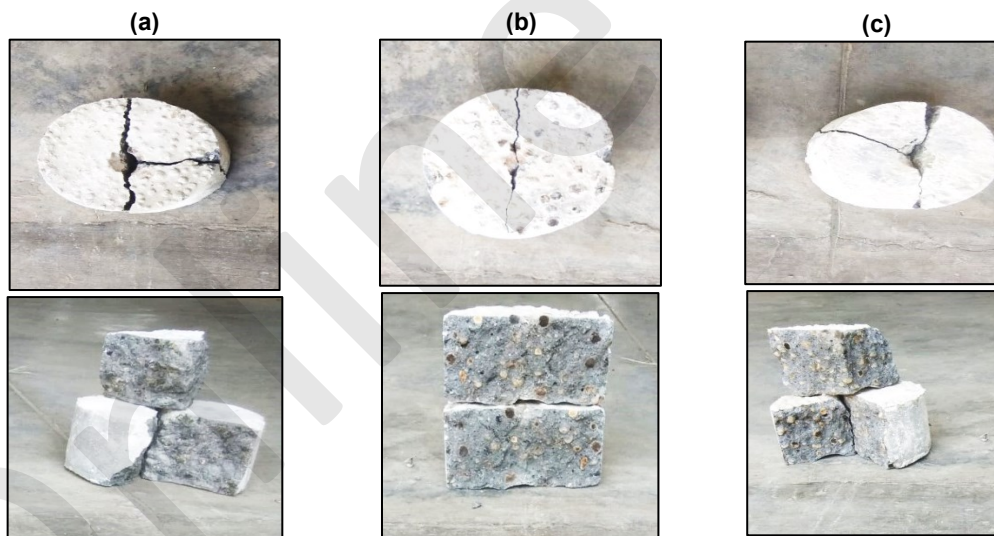


Figure 18. Failure modes of tested concrete mix with varying SFA (a) 0 % (b) 50 % (c) 100 %

3.8 Sorptivity (S)

By measuring the capillary rise absorption rate of the homogenous material, the sorptivity of the concrete mix can be determined. Water in this experiment was used to investigate the phenomenon of capillary action. Figure 19 depicts the test setup for measuring sorptivity on the concrete specimens. To prevent water from moving laterally within the disc, a non-absorbent (epoxy) applied coating was to its side, keeping the water level at no more than 3 mm above the specimen. The following formulas were used to calculate the sorptivity (S), and estimated for 30 minutes [47].

$$S = \frac{l}{\sqrt{t}} \text{ (mm/min}^{0.5}\text{)},$$

whereas

I define rate absorption as $\frac{w_2 - w_1}{Ad}$,

t = time in minutes,

w₁ = oven dry weight of specimen in kg,

w₂ = weight of specimen after 30 minutes of capillary suction of water in kg.

A is the surface area in which the water penetrates, and d is the density of water in kg/mm³. Table 7 displays the sorptivity results.



Figure 19. Test Setup for Sorptivity of Concrete Cylindrical Specimens

Table 7. Sorptivity ($10^{-2} \text{ mm/min}^{0.5}$) for Concrete Mix for SFA Content

Mix Designation	W1 (kg)	W2 (kg)	Surface Area (mm^2)	Density of water (kg/mm^3)	Sorptivity value ($10^{-2} \text{ mm/min}^{0.5}$)	Average sorptivity value ($10^{-2} \text{ mm/min}^{0.5}$)
SFA0-a	1.069	1.071	9424.77	10^{-6}	0.039	0.068
SFA0-b	1.042	1.047	9424.77	10^{-6}	0.097	
SFA50-a	1.164	1.167	9424.77	10^{-6}	0.058	0.058
SFA50-b	1.128	1.131	9424.77	10^{-6}	0.058	
SFA100-a	0.905	0.908	9424.77	10^{-6}	0.058	0.068
SFA100-b	0.861	0.865	9424.77	10^{-6}	0.077	

a & b indicate the first and second specimens respectively taken for the sorptivity test

The average findings reveal that incorporating 50% SFA in the concrete mix correlates with a reduction in sorptivity. Furthermore, the sorptivity value of concrete with 0% SFA matches that of concrete with 100% SFA. Partially substituting 50% SFA in concrete leads to a decrease in sorptivity. As per Gomathi et al. 2015 [16], maintaining SFA content within a specified range enhances the durability of the concrete mix. Additionally, M-sand proves to be a superior alternative to river sand in concrete applications.

4 Conclusions

The following conclusions were made based on the results of the previously mentioned experimental examinations:

- The introduction of M-sand into concrete leads to a decreased slump, while the inclusion of SFA results in an increased slump.
- The SFA100 concrete blend demonstrates lightweight properties, as evidenced by its wet density being 20% lower compared to concrete containing natural aggregates (SFA0). Similarly, the SFA100 mix had a 19% lower dry density than the SFA0 mix.
- With higher SFA content, mechanical characteristics such as compressive strength, split tensile strength, flexural strength, and Young's modulus decreased. However, comparing these three mixes was impractical due to variations in their dry and wet densities.

- According to IS 456 code, the minimum compressive strength required for concrete in the field is 20 MPa. Hence, SFA incorporation renders the concrete suitable for field applications while reducing the structure's self-weight.
- The partial replacement of SFA with natural coarse aggregates (NCA) affected the impact strength of the SFA50 concrete mix. During impact strength testing, both SFA 0 and SFA 100 concrete mixes failed in similar manners.
- The average sorptivity value indicates that replacing 50% of the NCA in concrete with SFA improves the concrete mix's durability.

Declarations:

Fundings: No funds, grants, or other support were received.

Conflicts of interest or competing interests: The authors declare that they have no known competing financial interests or personal relationships that could have appeared to influence the work reported in this paper.

CRedit authorship contribution statement: **Ranjith Babu B:** Conceived, planned the experiments and carried out the experiments. **Divyah N:** Analysis of the results and writing of the manuscript.

Acknowledgements: The author extends gratitude to Professor Dr. R. Thenmozhi, Head of the Civil Engineering Department at Government College of Technology in Coimbatore, for invaluable guidance. Acknowledgment is also due to Professor Dr. P. Velumani, Head of the Civil

Engineering Department at PSNA College of Engineering and Technology in Dindigul, for facilitating laboratory testing. We also extend special thanks to Mr. S. Murgesan, a structural engineering lab technician, for his invaluable assistance during laboratory experiments.

References

- [1]. Bentur, A., Igarashi, S. I., & Kovler, K. (2001). Prevention of autogenous shrinkage in high-strength concrete by internal curing using wet lightweight aggregates. *Cement and concrete research*, 31(11), 1587-1591. [https://doi.org/10.1016/S00088846\(01\)00608-1](https://doi.org/10.1016/S00088846(01)00608-1).
- [2]. Shelke, A. S., Ninghot, K. R., Kunjekar, P. P., & Gaikwad, S. P. (2014). Coconut shell as partial replacement for coarse aggregate. *International Journal of Civil Engineering Research*, 5(3), 211-214. https://www.ripublication.com/ijcer_spl/ijcerv5n3spl_02.pdf.
- [3]. Noaman, A. T., Jameel, G. S., & Ahmed, S. K. (2020). Producing of workable structural lightweight concrete by partial replacement of aggregate with yellow and/or red crushed clay brick (CCB) aggregate. *Journal of King Saud University-Engineering Sciences*. <https://doi.org/10.1016/j.jksues.2020.04.013>.
- [4]. <https://www.nbmcw.com/equipment-machinery/construction-equipments/concrete-equipment/sintered-fly-ash-light-weight-aggregate-production.html>.
- [5]. Shen, W., Liu, Y., Wang, Z., Cao, L., Wu, D., Wang, Y., & Ji, X. (2018). Influence of manufactured sand's characteristics on its concrete performance. *Construction and Building Materials*, 172, 574-583. <https://doi.org/10.1016/j.conbuildmat.2018.03.139>.
- [6]. Lo, Tommy & Tang, Waiching & Cui, Hongzhi. (2007). The effects of aggregate properties on lightweight concrete. *Building and Environment*. 42. 3025-3029. <https://doi.org/10.1016/j.buildenv.2005.06.031>.
- [7]. Revilla-Cuesta, V., Faleschini, F., Zanini, M. A., Skaf, M., & Ortega-Lopez, V. (2021). Porosity-based models for estimating the mechanical properties of self-compacting concrete with coarse and fine recycled concrete aggregate. *Journal of Building Engineering*, 44, 103425. <https://doi.org/10.1016/j.jobe.2021.103425>
- [8]. Malysheva, T. & Pavlov, R. (2012). Influence of the mineralogical composition of binders on the strength of sinter. *Steel in Translation*. 42. <https://doi.org/10.3103/S096709121211006X>.
- [9]. Qifeng Song, Ming-Zhi Guo, Tung-Chai Ling, (2022) A review of elevated-temperature properties of alternative binders: Supplementary cementitious materials and alkali-activated materials, *Construction and Building Materials*, Volume 341, 127894, <https://doi.org/10.1016/j.conbuildmat.2022.127894>.
- [10]. Manikandan, R. & K, Ramamurthy. (2012). Physical characteristics of sintered fly ash aggregate containing clay binders. *Journal of Material Cycles and Waste Management*. 14. <https://doi.org/10.1007/s10163-012-0045-1>.
- [11]. Kang Hoon Lee, Jae Hoon Lee, Young Min Wie, Ki Gang Lee, (2019), "Bloating Mechanism of Lightweight Aggregates due to Ramping Rate", *Advances in Materials Science and Engineering*, vol. 2019, 12 pages. <https://doi.org/10.1155/2019/2647391>.
- [12]. Tang, Chao-Wei. (2022). The Temperature and Pore Pressure Distribution of Lightweight Aggregate Concrete Slabs Exposed to Elevated Temperatures. *Applied Sciences*. 12. 10317. <https://doi.org/10.3390/app122010317>.
- [13]. Yuan Gao, Gao Liu, Xiao Han, Quanqing Gao, Jinghua Ren, (2024), Research on the design method of mix proportion of ceramsite lightweight aggregate concrete, *Construction and Building Materials*, Volume 433, 136665, <https://doi.org/10.1016/j.conbuildmat.2024.136665>.
- [14]. Jiwei Cai, Zixian Liu, Gelong Xu, Qing Tian, Weiguo Shen, Bowang Li, Tiao Chen, (2022), Mix design methods for pervious concrete based on the mesostructure: Progress, existing problems and recommendation for future improvement, *Case Studies in Construction Materials*, Volume 17, <https://doi.org/10.1016/j.cscm.2022.e01253>.
- [15]. T.Y. Lo, H.Z. Cui, (2004), Effect of porous lightweight aggregate on strength of concrete, *Materials Letters*, Volume 58, Issue 6, Pages 916-919, <https://doi.org/10.1016/j.matlet.2003.07.036>.
- [16]. Sivakumar, A., & Gomathi, P. (2012). Pelletized fly ash lightweight aggregate concrete: A promising material. *Journal of Civil Engineering and Construction Technology*, 3(2), 42 - 48. <https://doi.org/10.5897/JBD11.088>.
- [17]. Lo, T. Y., Cui, H., Memon, S. A., & Noguchi, T. (2016). Manufacturing of sintered lightweight aggregate using high-carbon fly ash and its effect on the mechanical properties and microstructure of concrete. *Journal of Cleaner Production*, 112, 753-762. <https://doi.org/10.1016/j.jclepro.2015.07.001>.
- [18]. Satpathy, H. P., Patel, S. K., & Nayak, A. N. (2019). Development of sustainable lightweight concrete using fly ash cenosphere and sintered flyash aggregate. *Construction and Building Materials*, 202, 636-655. <https://doi.org/10.1016/j.conbuildmat.2019.01.034>.
- [19]. Babu, B. R., & Thenmozhi, R. (2018). An investigation of the mechanical properties of sintered fly ash lightweight aggregate concrete (SFLWAC) with steel fibers. *Archives of Civil Engineering*, 64(1). https://journals.pan.pl/Content/115555/PDF/05_073-085_ace-2018-0005.pdf.
- [20]. Shen, W., Liu, Y., Cao, L., Huo, X., Yang, Z., Zhou, C., ... & Lu, Z. (2017). Mixing design and microstructure of ultra-high strength concrete with manufactured sand. *Construction and Building Materials*, 143, 312-321. <https://doi.org/10.1016/j.conbuildmat.2017.03.092>.
- [21]. Akarsh, P. K., Marathe, S., & Bhat, A. K. (2021). Influence of graphene oxide on properties of concrete in the presence of silica fumes and M-sand. *Construction and Building Materials*, 268, 121093. <https://doi.org/10.1016/j.conbuildmat.2020.121093>.
- [22]. Pilegis, M., Gardner, D., & Lark, R. (2016). An investigation into the use of manufactured sand as a 100% replacement for fine aggregate in concrete. *Materials*, 9(6), 440. <https://www.mdpi.com/142616>.
- [23]. IS: 12269, Indian Standard Specification 53 Grade ordinary Portland cement specification, Bureau of Indian Standards, New Delhi, 1987 [Reaffirmed in 2013].
- [24]. IS: 4031, Indian Standard Specification, Methods of Physical Tests for Hydraulic Cement: Part 11, Determination of Density, Bureau of Indian Standards, New Delhi, 1988 [Reaffirmed in 2005].

- [25]. IS: 4031, Indian Standard Specification, Methods of Physical Tests for Hydraulic Cement: Part 2, Determination of Fineness by Specific Surface by Blaine Air Permeability Method, Bureau of Indian Standards, New Delhi, 1999[Reaffirmed in 2004].
- [26]. IS: 4031, Indian Standard Specification, Methods of Physical Tests for Hydraulic Cement: Part 4, Determination of Consistency of Standard Cement Paste, Bureau of Indian Standards, New Delhi, 1988 [Reaffirmed in 2005].
- [27]. IS: 4031, Indian Standard Specification, Methods of Physical Tests for Hydraulic Cement: Part 5, Determination of Initial and Final Setting Times, Bureau of Indian Standards, New Delhi, 1988 [Reaffirmed in 2005].
- [28]. IS: 2386, Indian Standard Specification, Methods of Test for Aggregates for Concrete: Part 1, Particle Size and Shape, Bureau of Indian Standards, New Delhi, 1963 [Reaffirmed in 2002].
- [29]. IS: 2386, Indian Standard Specification, Methods of Test for Aggregates for Concrete: Part 3, Specific Gravity, Density, Voids, Absorption and Bulking, Bureau of Indian Standards, New Delhi, 1963 [Reaffirmed in 2002].
- [30]. IS: 2386, Indian Standard Specification, Methods of Test for Aggregates for Concrete: Part 4, Mechanical Properties Bureau of Indian Standards, New Delhi, 1963 [Reaffirmed in 2002].
- [31]. IS: 10500, Indian Standard, Drinking Water – Specification, Bureau of Indian Standards, New Delhi (2012).
- [32]. IS: 10262. Indian Standard Concrete Mix Proportioning – Guidelines, Bureau of Indian Standards, New Delhi; 2009.
- [33]. IS: 516, Indian Standard Methods of Tests for Strength Concrete, Bureau of Indian Standards, New Delhi, 1959 [Reaffirmed in 1999].
- [34]. IS: 5816, Indian Standard Splitting Tensile Strength of Concrete-Method of Test, Bureau of Indian Standards, New Delhi, 1999 [Reaffirmed in 2004].
- [35]. ASTM C 642-13, Standard Test Method for Density, Absorption, and Voids in Hardened Concrete, ASTM International, West Conshohocken, 2013.
- [36]. ASTM C 1585-04, Standard Test Method for Measurement of Rate of Absorption of Water by Hydraulic Cement Concretes.
- [37]. ACI Committee 213, 213R-03, Guide for Structural Lightweight-aggregate Concrete, American Concrete Institute, Farmington Hills, MI, USA, 2003.
- [38]. American Concrete Institute, ACI Committee 318: Building Code Requirements for Structural Concrete, Farmington Hills, MI, 2011.
- [39]. CEB-FIP, Model Code 1990. Com, Euro-International Du Beton, Paris, 1991.
- [40]. EHE, Spanish Code for Structural Concrete EHE, Real Decreto 2661/1998, Madrid, 1998.
- [41]. GB: 10010, Code for Design of Concrete Structures, Chinese Standard, Beijing (China), 2002.
- [42]. NBR 6118, Design of Concrete Structures, Brazilian association of technical standards, Brazil, 2003.
- [43]. A.M. Neville, Properties of Concrete, 5th ed., Person Education Limited, New Delhi, 2013.
- [44]. DG/TJ, Technical Code for Application of Recycled Aggregate Concrete, Shanghai Construction Standard Society (SCSS), Shanghai, 2008.
- [45]. IS: 456, Indian Standard Plain and Reinforced Concrete Code of Practice, Bureau of Indian Standards, New Delhi, 2000.
- [46]. ACI 544-2R, Measurement of Properties of Fiber Reinforced Concrete, American Concrete Institute, USA (1999).
- [47]. Jena, T., & Panda, K. C. (2020). Effect of magnesium sulphate solution on compressive strength and sorptivity of blended concrete. *Advances in concrete construction*, 9(3), 267-278. <https://doi.org/10.12989/acc.2020.9.3.267> .
- [48]. 36. Gupta, T., Sharma, R. K., & Chaudhary, S. (2015). Impact resistance of concrete containing waste rubber fiber and silica fume. *International Journal of Impact Engineering*, 83, 76-87. <https://doi.org/10.1016/j.ijimpeng.2015.05.002>